Minerals **2015**, *5*, 221-246; doi:10.3390/min5020221

OPEN ACCESS

minerals

ISSN 2075-163X

www.mdpi.com/journal/minerals

Article

Approaches to the Low Grade Metamorphic History of the Karakaya Complex by Chlorite Mineralogy and Geochemistry

Sema Tetiker [1], Hüseyin Yalçın [2,*] and Ömer Bozkaya [3]

[1] Department of Geological Engineering, Batman University, 72100 Batman, Turkey; E-Mail: sema.tetiker@batman.edu.tr

[2] Department of Geological Engineering, Cumhuriyet University, 58140 Sivas, Turkey

[3] Department of Geological Engineering, Pamukkale University, 20070 Denizli, Turkey; E-Mail: obozkaya@pau.edu.tr

* Author to whom correspondence should be addressed; E-Mail: yalcin@cumhuriyet.edu.tr; Tel.: +90-0542-412-16-19.

Academic Editor: Antonio Simonetti

Received: 18 November 2014 / Accepted: 9 April 2015 / Published: 16 April 2015

Abstract: In this study, chlorite is used to investigate the diagenetic-metamorphic evolution and accurate geological history of the different units belonging to the Karakaya complex, Turkey. Primary and secondary chlorite minerals in the very low-grade metamorphic rocks display interference colors of blue and brown and an appearance of optical isotropy. Chlorites are present in the matrix, pores, and/or rocks units as platy/flaky and partly radial forms. X-ray diffraction (XRD) data indicate that Mg-Fe chlorites with entirely IIb polytype (trioctahedral) exhibit a variety of compositions, such as brunsvigite-diabantite-chamosite. The major element contents and structural formulas of chlorite also suggest these were derived from both felsic and metabasic source rocks. Trace and rare earth element (REE) concentrations of chlorites increase with increasing grade of metamorphism, and these geochemical changes can be related to the tectonic structures, formational mechanics, and environments present during their generation.

Keywords: petrography; XRD; major and trace elements; geological evolution

1. Introduction

Chlorite is a typical rock-forming mineral present in very low grade facies of metamorphic rocks. Chlorite may originate from aggradation (positive transformation) following the evolution of neomineralization of trioctahedral smectite → interlayered smectite-chlorite (C-S) → chlorite, which implies prograde metamorphism due to burial and subsequent diagenesis. Moreover, it represents degradation (negative transformation) in igneous rocks from trioctahedral mica and ferromagnesian minerals, and residual and authigenic minerals in sedimentary rocks [1]. The most significant mineralogical and chemical changes/transformations in chlorite occur during burial diagenesis/metamorphism (e.g., [2–13]). The fact that the half-height width of the 7-Å chlorite peak [14] decreases with the increasing diagenetic/metamorphic grade has been used as a mineralogical parameter for the determination of the diagenetic/metamorphic grade; in particular for metabasic (metavolcanic) rocks, despite these not being as widespread as illites (e.g., [15–18]).

Chlorite occurs pervasively in the various units of the Karakaya Complex, one of the most debated tectonic settings within Turkey [19–21]. In this study, the utility of chlorite is demonstrated relative to the interpretation of the diagenetic-metamorphic evolution of the different units within the Karakaya complex.

2. Geotectonic Setting and Lithology

The Karakaya Complex [22] within the Sakarya Tectonic Unit [23] consists of units representing the remnants of the subduction accretionary prism formed by the closure of the Pre-Jurassic Paleotethys Ocean [24,25]. It is divided into two areas [26] (Figure 1) with the Lower Karakaya Complex (LKC), identified as the Nilüfer unit in northwestern Anatolia and Turhal Metamorphites in the central NE Anatolia [27,28]; this unit is structurally and stratigraphically located at the bottom, and consists of rocks subjected to metamorphism at the end of the Paleozoic or during the Triassic [24]. The LKC units are divided into the upper and lower (LKC-LP and LKC-UP) parts in accordance with their petrographic properties and the mineralogy of phyllosilicates, which correspond to blueschist and greenschist facies, respectively [21]. These are represented by metapsammite (metasandstone), metapelites (slate, phyllite, schist), metacarbonates (metalimestone, metadolomite, marble), and metabasic rocks (metavolcanic, metatuff) in NW Anatolia, and metapelitic (phyllite, slate, metasiltstone), metasandstone, metamagmatic (metabasalt, metatuff, metagabbro, metadiabase), and metalimestone in the central NE Anatolia region.

The Upper Karakaya Complex (UKC) contains many exotic limestone blocks within the Permo-Carboniferous-aged units [29–31]. It consists mainly of three units (Hodul, Orhanlar and Çal) of Permian or Triassic age that is strongly deformed in the NW Anatolia [24] and Devecidağ Melange [27] in the central NE Anatolia. Among these, the Hodul unit comprises arkosic sandstones and intercalated (meta-) pelitic rocks (mudstone, shale, slate, siltstone); the Orhanlar unit contains shale intercalated sandstones; the Çal unit consists of spilitic basaltic lava-agglomerates and clastic rocks (mudstone, shale, sandstone); and the Devecidağ Melange unit contains metapelitic rocks (metashale, slate, metasiltstone), metasandstone, spilitic metabasalt, and metalimestones.

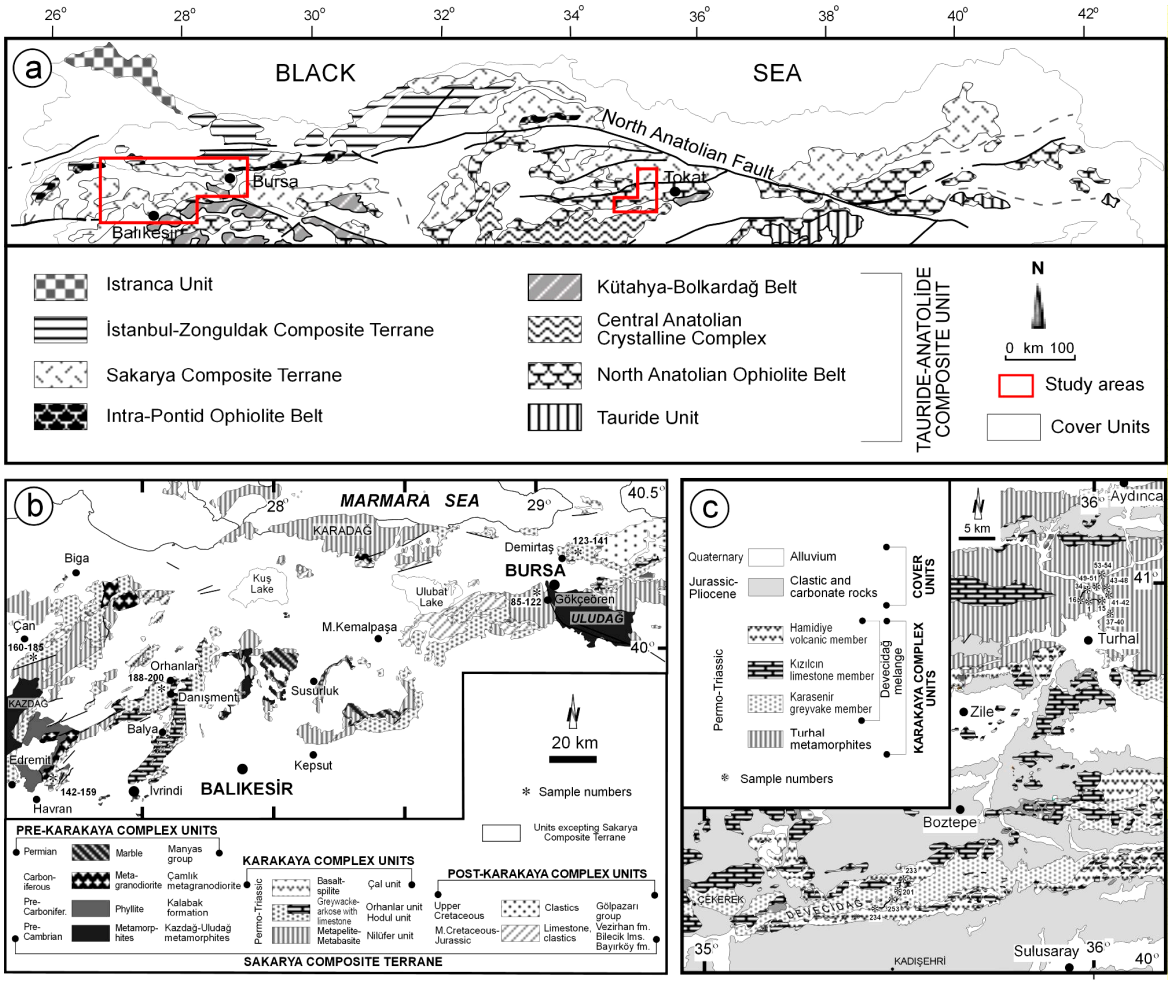

Figure 1. Simplified geologic-geotectonic maps of the Karakaya Complex and related units (unit boundaries [32] and unit determinations [23], (**a**) The Alpine tectonic units of northern Turkey (unit boundaries [32]; (**b**) NW Anatolia (modified after MTA [32]); (**c**) Central NE Anatolia [27].

3. Materials and Methods

In total, 253 rock samples were taken from various units within the area of investigation. The weathered surface and soil on the samples were removed by crushing and then washing with ultrapure water. Subsequently, samples underwent various processes such as thin sectioning, crushing–grinding–screening, clay separation, X-ray diffraction (XRD), and optical microscopy (OM) at Cumhuriyet University (CU), Department of Geology and Mineralogy-Petrography and Geochemistry Research Laboratories (MİPJAL). Scanning electron microscopy (SEM) was conducted at the Turkish Petroleum Corporation Research Center (Ankara).

The samples investigated by XRD were first crushed in pieces of 3–5 cm in diameter with a hammer and then into fine particles (<5 mm) in a Fritisch rock crusher. Depending on their hardness, samples were then ground for 10–30 min in a silicon carbide bowl grinder and/or agate mortar. The powder material was then placed in plastic bags and labeled and ready for analysis. The XRD analyses were conducted with a DMAX III X-ray diffractometer (Rigaku Corporation, Tokyo, Japan) (Anode = Cu (Cu Kα = 1.541871 Å), Filter = Ni, Voltage = 35 kV, Current = 15 mA, Gonimeter speed = 2°/min,

Paper speed = 2 cm/min, Time constant = 1 s, Slits = 1°–0.15 mm–1°–0.30 mm, Paper interval 2θ = 5°–35°).

As a result of the XRD analyses, all rock and clay-sized components (<2 μm) of the samples were defined and their semi-quantitative percentages were calculated using the external standard method [33]. Mineral intensity factors were used in all rock and clay fraction calculations and the reflections were measured in mm. In this method, kaolinite was taken as a reference from the glycolylated preparations for clay fraction and dolomite for whole rock [34]. Quartz was used as the internal standard in the measurement of d-spaces. The definitions of clay minerals were based mainly according to their (001) basal reflections.

The separation of phyllosilicate/clay minerals was conducted at the Clay Separation Laboratory, Department of Geological Engineering, Cumhuriyet University. The clay separation process necessary for the XRD-CF analyses essentially consists of chemical solving (removal of non-clay fraction), centrifugation–decantation/resting and washing, suspending–sedimentation–siphoning–centrifugation, and bottling. In the absence of suspended particles, the separation process was accelerated by the addition of Calgon. Centrifugation was performed using a Sepatech Varifuge 3.2S (Heraeus Group, Frankfurt, Germany) model centrifuger at 5600 cycles/min speed and 200 cc capacities with stainless steel and/or plastic bowls. Three oriented slide preparations from each clay mud were prepared as plastering, or in suspension and these were dried at room temperature. Clay fraction diffractograms were obtained by putting through the processes of normal-AD (air-dried), glycolylated-G (leaving in ethylene glycol vapour in a dessicator for 16 h at 60 °C) and heated-H (heating in the oven for 4 h at 490 °C). The goniometer speed at the intervals was set at 1°/min and the recording interval was set as 2θ = 2–30° (±0.04°).

In the measurement of the illite crystallinity, the width at the half-height of the 10-Å illite peak Δ°2θ (Kübler index—[35,36]) was used. The peak widths were calibrated according to Kisch [37] and Warr and Rice [38] standards. WINFIT [39] programme (http://xray.geol.uni-erlangen.de/html/software/soft.html) was used to distinguish the single and two illite phases with the asymmetric and symmetric peaks as well as crystalline illite-WCI and poor crystalline illite-PCI. For the lower and upper limits of the anchizone, 0.21 and 0.37 Δ°2θ, and 0.25 and 0.42 Δ°2θ were taken respectively for Kisch [37,40] and CIS [38] standards.

In the measurement of chlorite "crystallinity", the half-height width (Δ°2θ; Árkai index—AI: [15,36]) of 7-Å chlorite peak was used. The diagenesis-anchizone and anchizone-epizone limits for AI were suggested as 0.37 and 0.26 (Δ°2θ) respectively [15–17]; and according to the Kübler index (KI; [35]) limits (0.42 and 0.25 Δ°2θ), the anchizone-epizone limit is similar, while the diagenesis-anchizone limit is lower. WINFIT [39] programme was used for precise determination of peak widths. Polytype examinations in chlorite minerals were performed between the recording interval of 2θ = 31°–52° as from the nonoriented plaques. Diagnostic peaks suggested by Bailey [41] were used in the determination of the polytypes.

The following method was used in order to determine the chemical components of the chlorites: $d_{(001)}$ reflection values were found as from $d_{(005)}$ peaks and the amount of tetrahedral Al was established according to $d_{(001)} = 14.55\ Å - 0.29Al^{IV}$ formula [42]. The amount of octahedral Fe^{2+} was obtained from the diagram using the $[I_{(002)} + I_{(004)}]/[I_{(001)} + I_{(003)}]$ [43] and $I_{(002)}/I_{(001)}$ and $I_{(004)}/I_{(003)}$ [44] ratios. In this method, the Fe contents in the talc and brucite layers can be determined with the help of

the $I_{(004)}/I_{(003)}$ ve $I_{(002)}/I_{(001)}$ basal peak ratios of the chlorite minerals. Mg contents were determined in accordance with the Fe + Al^{VI} + Mg = 6 equation by presuming that $Al^{IV} = Al^{VI}$.

The major, trace, and rare earth element (REE) analyses of four pure (or nearly pure) chlorite fractions were performed at Activation Laboratories Ltd. (Actlabs, Ancaster, ON, Canada). Fusion inductively coupled plasma (ICP) was used for major element analysis, while inductively coupled plasma-mass spectrometry (ICP-MS) was employed for the analyses of trace and REEs. Details of the analysis method and the instrument detection limits are provided on Actlabs' website (http://www.actlabs.com/).

4. Results

4.1. Petrography

4.1.1. Optical Microscope Examinations

Plagioclase microliths are present in microlithic porphyritic metavolcanic rocks representing the Nilüfer Unit within the LKC-LP in NW Anatolia. The groundmass material consists mainly of volcanic glass, phyllosilicates, and amphiboles. The volcanic glass within the matrix has been subjected to mainly chloritization, silicification and partly Fe-oxidation, and carbonization. Chlorite minerals show blue and brown interference colors, but are mainly green in plane polarized light. Chlorite plates oriented parallel to the crystallographic c-axis and quartz-rich zones that are sequenced in the direction of c-crystallographic axis in the blue schists {001} of the Nilüfer Unit (LKC-LP), and are typical textures indicative of metamorphic differentiation (Figure 2a). Isotropiclike chlorite minerals in the matrix are observed in porphyroblasts that form in tremolite-rich metabasalts of the LKC-UP, which formed under greenschist facies conditions (Figure 2b).

Platy chlorite minerals (displaying blue interference color) result from the neoformation within greenschist facies metasandstones defined as Turhal Metamorphites of LKC-UP in the central NE Anatolia. Muscovite, biotite, and chlorite stack (pod) structures showing micro-orientation and bending in certain metasandstones are typical. The stacks look platy/flaky, and partly radial, and these have three different mineralogical compositions that are chlorite-muscovite (CMS), chlorite-biotite (CBS), and biotite-muscovite (BMS) stacks (Figure 2c). In metavolcanic rocks, green chlorite minerals are characterized by blue and brown interference colours. The chlorites in the matrix and pores may also show optical isotropic-like features as in corresponding rocks in NW Anatolia (Figure 2d).

The chlorites in the pores of sandstones in the Orhanlar Unit among UKC units in NW Anatolia display a blue interference colour (Figure 3a,b). Chlorite has a distinctive reaction rim that indicates retrograde metamorphism. Furthermore, calcite and rare epidote minerals are other components in the pores. Volcanic rocks constituting the main lithology of the Çal Unit have hypocrystaline porphyritic, vitrophyric-microlitic porphyritic, amygdaloidal, and partly glomeroporfiric textures. The groundmass consists of plagioclase microlites and mostly chloritized volcanic glass (Figure 3c).

The groundmass for the metasandstones from the Devecidağ Melange among UKC units in the central NE Anatolia consists of Fe oxidation and phyllosilicates matrix in addition to calcite and/or dolomite and silica cement. Chlorite minerals are typically observed with blue interference color developed within pores and matrix (Figure 3d).

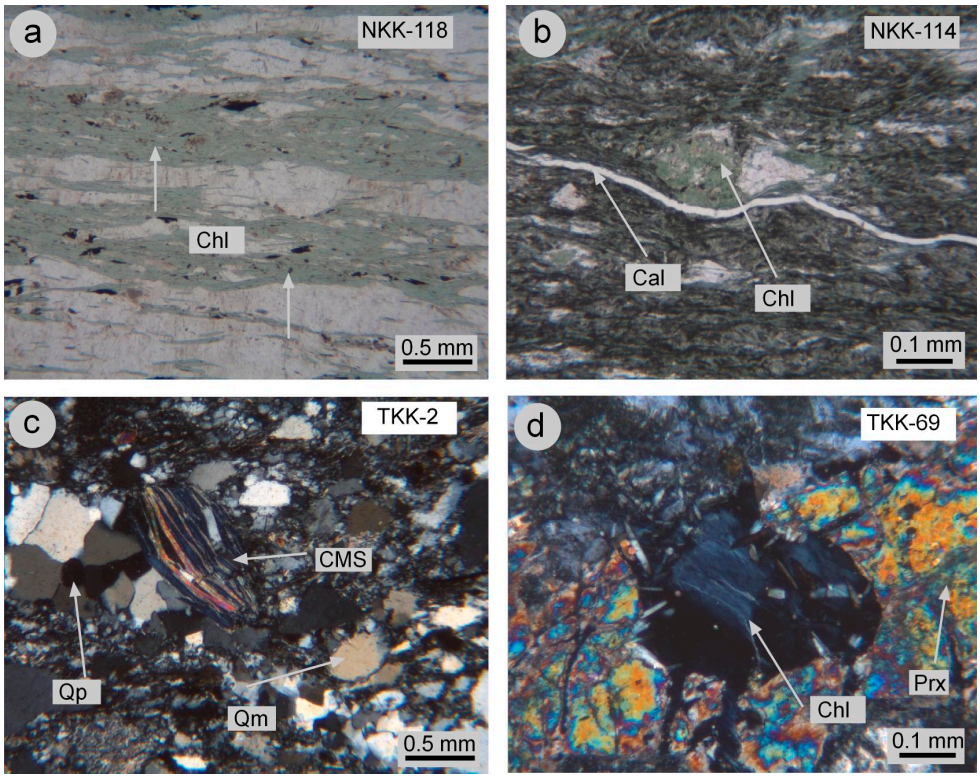

Figure 2. Optical microphotograps of chlorite and associated minerals in the Lower Karakaya Complex units (Chl = Chlorite, Qp = Polycrystalline quartz, Qm = Monocrystalline quartz, CMS = Chlorite-muscovite stack, Cal = Calcite, Prx = Pyroxene, ppl = plane polarized light, cn = crossed polars); (**a**) Typical metamorphic differentiation in the schists of the Nilüfer Unit (ppl); (**b**) Isotropic-view chlorite porphyblasts and pore filling calcite occurrences within the matrix with oriented texture of tremolitized metabasalts from Nilüfer Unit (ppl); (**c**) Monocrystalline and polycrystalline quartzs, and chlorite-muscovite stack in the metasandstones of Turhal Metamorphites (cp); (**d**) Blue interference colored chlorites within the metabasalts of Turhal Metamorphites (cp).

4.1.2. Scanning Electron Microscopy

The greenschist facies sample of shale (NKK-93) from the Nilüfer Unit, LKC-UP in NW Anatolia consists of chlorite, illite, quartz, feldspar, and calcite, with chlorite minerals forming clusters in the form of plates (Figure 4a). The illites are mainly in the form of parallel, partly radially sequenced long and thin filaments (2–30 μm) (Figure 4b).

In the greenschist facies metasandstone sample (NKK-93) of the Turhal Metamorphites, LKC-UP in central NE Anatolia comprises illite, chlorite, quartz, and feldspar, with the chamosite Fe-chlorites occurring as thick platy forms (Figure 4c). The illites range between 10–50 μm in length and are observed in part as thin filamentous balls (Figure 4d).

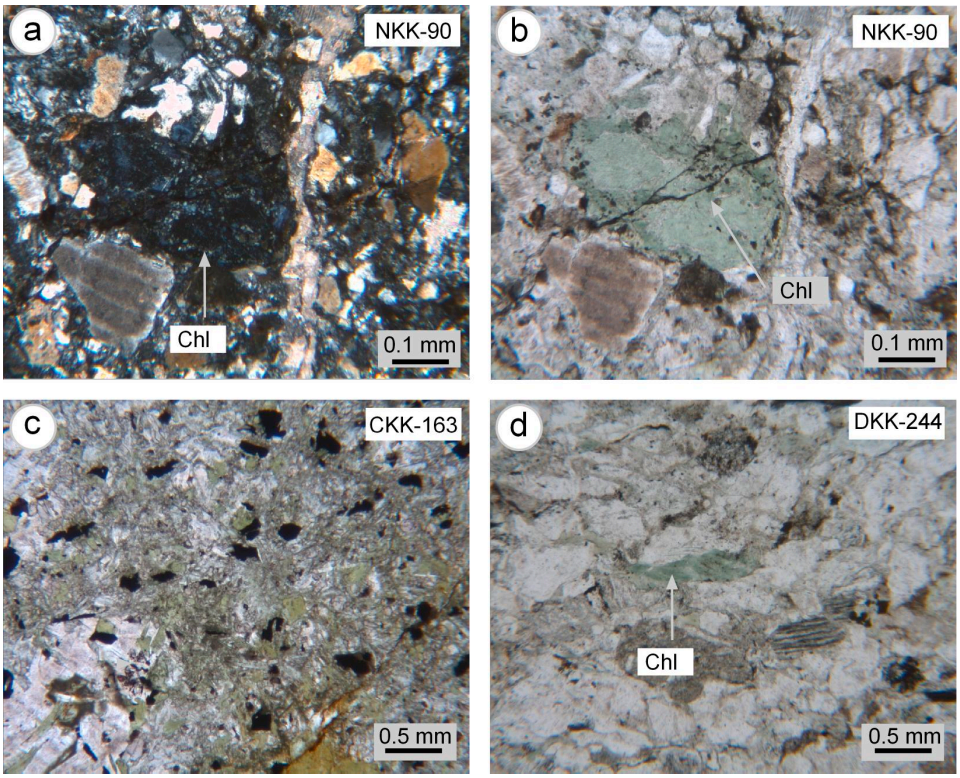

Figure 3. Optical microphotographs of chlorite and associated minerals from the Upper Karakaya Complex units (Chl = Chlorite, ppl = plane polarized light, cn = crossed polars); (**a**) Blue interference colored chlorite within the metasandstones of Orhanlar Unit (cp); (**b**) Green colored chlorite within the metasandstones of Orhanlar Unit (ppl); (**c**) Green colored chlorites within the metabasalts of Çal Unit (ppl); (**d**) Green colored chlorites within the metabasalts of Devecidağ Melange (ppl).

4.2. X-Ray Diffraction Mineralogy

4.2.1. Whole Rock and Clay Fraction

The mineralogical composition of rocks within the KC units is given in Table 1. Volcanogenic (feldspar, augite), metamorphic-metasomatic (glaucophane, tremolite/actinolite, epidote, stilpnomelane, phyllosilicates), and secondary minerals (calcite, dolomite, quartz, hematite, goethite) were recorded in metapelitic and metavolcanogenic rocks constituting the LKC-LP Nilüfer Unit in NW Anatolia. Phyllosilicate minerals consist of chlorite + illite unity and stilpnomelane, smectite and mixed-layer (C-S and C-V) minerals are involved in this unity to a lesser amount. In slate, chlorite wholly represents the clay fraction (Figure 5a).

Volcanogenic (feldspar), metamorphic-metasomatic (glaucophane, tremolite/actinolite, epidote, stilpnomelane, paragonite, phyllosilicates) and secondary chemical minerals (calcite, dolomite, quartz, hematite, goethite) were noted in metamagmatic and metapelitic rocks of LKC-LP Turhal Metamorphites in the central NE Anatolia. Pure chlorite (Figure 5b) represents the phyllosilicate mineral in metatuffites and the chlorite + illite association in the remaining rocks.

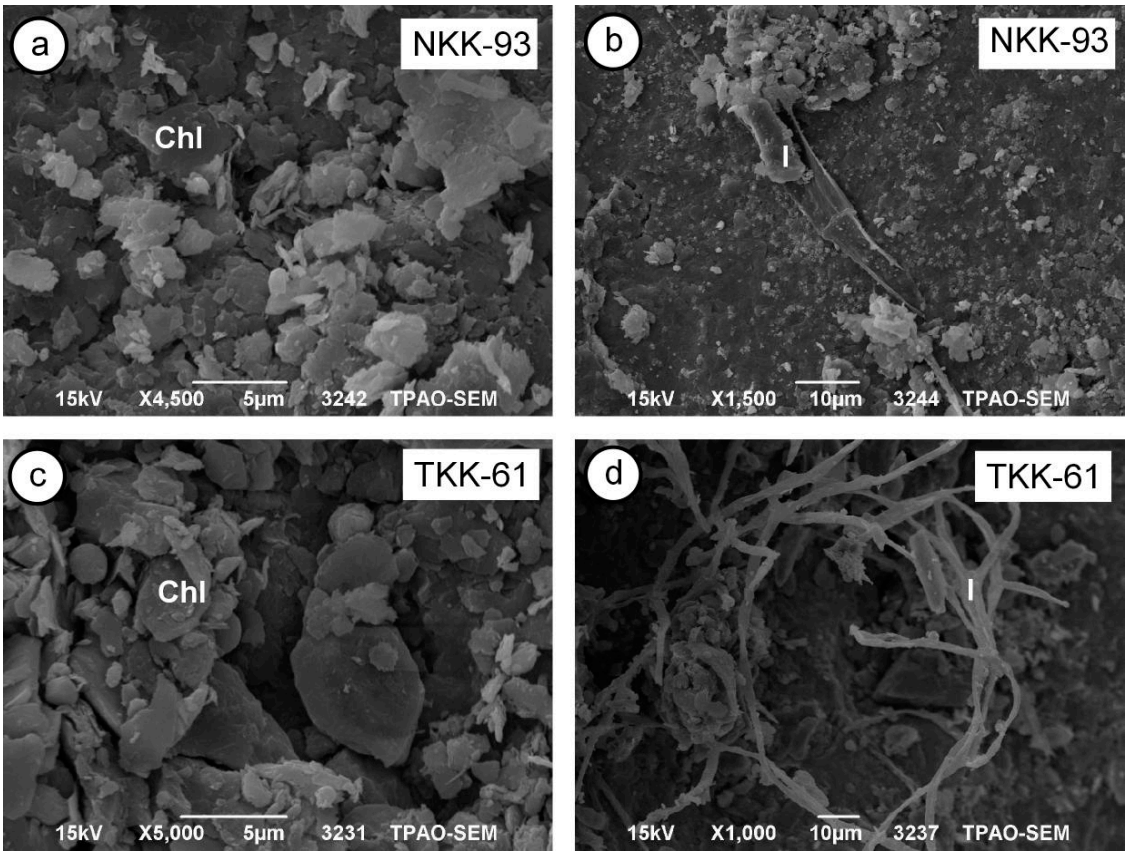

Figure 4. Scanning electron microscopy (SEM) photos of chlorite and associated minerals in the Lower Karakaya Complex units (Chl = Chlorite, I = Illite), (**a**) Platy chlorites in the shale sample of the Nilüfer Unit; (**b**) Thin-long filaments of illites in the shale sample of the Nilüfer Unit; (**c**) Radial needle-like chlorites and surrounding illites within the pores of metasandstones in the Turhal Metamorphites; (**d**) Fibrous illites in the metasandstones of the Turhal Metamorphites.

Table 1. The dominant mineralogy of samples from the Karakaya Complex (KC) units.

Unit	Area	KC	Facies	Minerals
Çal	NW Anatolia	UKC	Greenschist	chlorite, illite, C-V, C-S
Orhanlar				chlorite, illite, C-S, C-V, I-S, epidote
Hodul				illite, chlorite, I-S, C-V
Nilüfer		LKC-UP		augite, hornblende, epidote, stilpnomelane, illite, chlorite, C-S, C-V, I-S
		LKC-LP	Blueschist	glaucophane, tremolite/actinolite, augite, epidote, stilpnomelane, chlorite, illite, C-V, C-S
Devecidağ Melange	Central NE Anatolia	UKC	Greenschist	augite, epidote, prehnite, illite, chlorite, C-S, C-V, I-C, I-S
Turhal Metamorphites		LKC-UP		augite, epidote, illite, chlorite, paragonite, stilpnomelane, I-C, I-S, C-S, C-V
		LKC-LP	Blueschist	glaucophane, tremolite/actinolite, epidote, stilpnomelane, paragonite, illite, chlorite

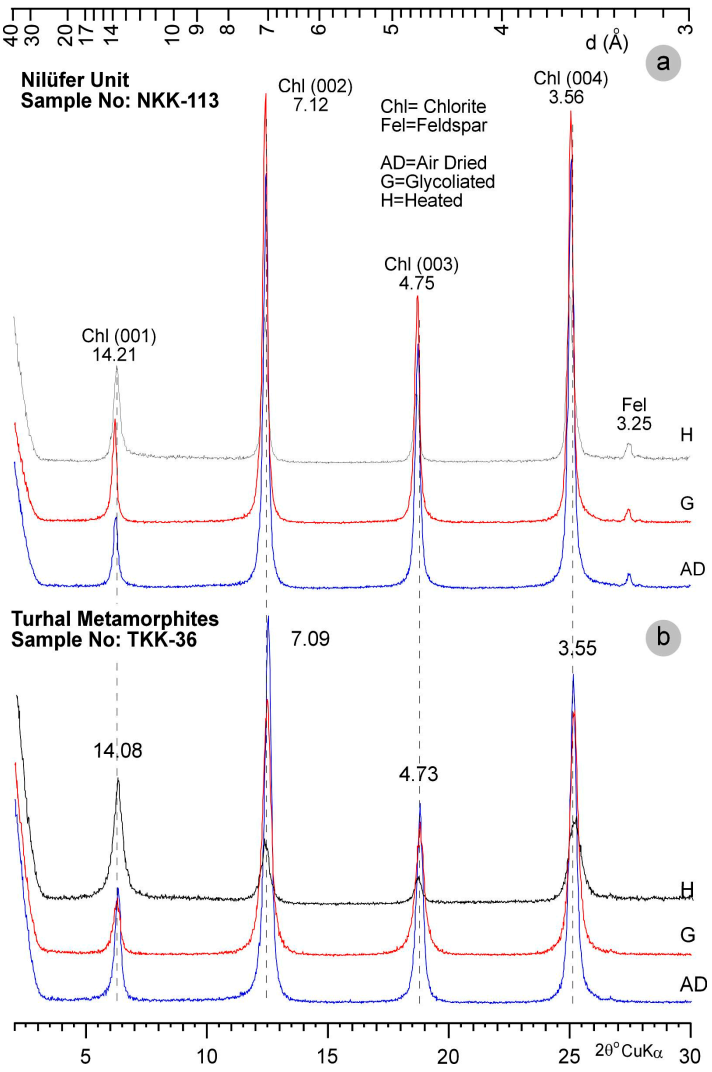

Figure 5. Oriented X-ray diffraction (XRD) patterns of chlorite minerals in the units of Lower Karakaya Complex-Lower Part, (**a**) Slate sample of blueschist facies in the Nilüfer Unit; (**b**) Metatuffite sample of greenschist facies in the Turhal Metamorphites.

Volcanogenic (pyroxene, feldspar), metamorphic-metasomatic (amphibole, epidote, stilpnomelane), and secondary minerals (calcite, dolomite, quartz, hematite, goethite) were detected in metapsammite, metapelite, metacarbonate, and metabasic rocks representing LKC-UP in NW Anatolia. While phyllosilicates are mostly represented by illite + chlorite paragenesis, in some instances this assemblage is accompanied by stilpnomelane, smectite, kaolinite, and mixed-layer (C-S, C-V and I-S) minerals.

Metapelitic, metapsammitic, metamagmatic, and metalimestones in LKC-UP in the central NE Anatolia contain feldspar, phyllosilicate, quartz, pyroxene, epidote, stilpnomelane, paragonite, calcite, dolomite, hematite, and goethite minerals. In these rocks, illite, chlorite, kaolinite, smectite, paragonite, stilpnomelane, and mixed layer (I-C, I-S, C-S and C-V) minerals represent phyllosilicates in the order of abundance. In these samples, illite + chlorite association constitutes the widespread phyllosilicate paragenesis. While the assemblage of illite + chlorite is observed in certain metasedimentary rocks, the association of chlorite + stilpnomelane was detected in metavolcanic rocks. Illite + kaolinite + smectite, illite + chlorite + paragonite + I-S and illite + chlorite + I-C or C-V assemblages constitute other parageneses.

Clastic rocks and (meta-) limestones of the Hodul Unit within the UKC in NW Anatolia contain quartz, phyllosilicate (illite, kaolinite, I-S, C-V, smectite and chlorite), calcite, and feldspar. Clastic rocks and (meta-) limestones of the Orhanlar Unit have quartz, feldspar, phillosilicate (chlorite, illite, C-S, C-V and I-S), calcite, and epidote minerals. Calcite, phyllosilicate (chlorite, C-S, vermiculite, illite and C-V), quartz, feldspar, hematite, and dolomite minerals were recorded in metavolcanic, shale and limestones of the Çal Unit.

Metapelitic, metapsammitic, metavolcanic, and metalimestones from the Devecidağ Melange within the UKC units in central NE Anatolia consist of quartz, feldspar, phyllosilicate (illite, chlorite, C-S, C-V, smectite, kaolinite, I-C and I-S), pyroxene, epidote, hematite, dolomite, and prehnite minerals.

4.2.2. Polytype

The results of polytype examinations of pure chlorite fractions for the Nilüfer unit in NW Anatolia and Turhal Metamorphites in the central NE Anatolia of the LKC are given in Table 2. It was detected that the chlorite associations of the LKC-LP and LKC-UP, which correspond to blueschist and greenschist facies in metavolcanic and metapelitic rocks of the Nilüfer Unit and Turhal Metamorphites are entirely of IIb polytype (Figure 6).

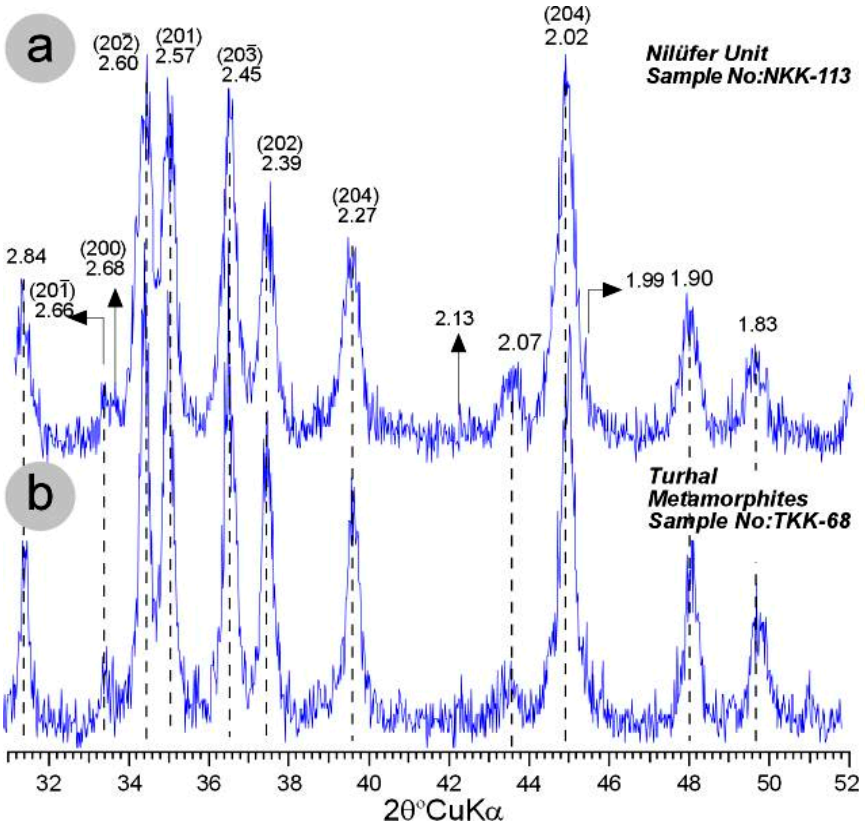

Figure 6. Unoriented XRD patterns of chlorite minerals in the units of Lower Karakaya Complex-Lower Part, (**a**) Slate sample of blueschist facies in the Nilüfer Unit; (**b**) Metagabbro sample of greenschist facies in the Turhal Metamorphites.

Table 2. The results of polytype examination of chlorite minerals in the Karakaya Complex units.

Unit	Area	KC	Facies	Sample No	Polytype	Lithology
Nilüfer	NW Anatolia	LKC-UP	Greenschist	NKK-103	IIb	Calcslate
		LKC-LP	Blueschist	-113	IIb	Slate
Turhal Metamorphites	Central NE Anatolia	LKC-UP	Greenschist	TKK-36	IIb	Metatuffite
				-58	IIb	Metagabbro
				-63	IIb	Metavolcanic
				-64	IIb	Metavolcanic
				-68	IIb	Metagabbro
				-73	IIb	Metabasalt
				-82	IIb	Phyllite

4.2.3. Composition

The chemical compositions of the chlorites for the LKC units determined in accordance with basal peak values and intensity ratios are listed in Tables 3 and 4 and shown in Figure 7. The reflection values of the (001) surface in the chlorites in NW Anatolia vary between 14.189–14.338 Å (14.249 Å on average) for LKC-LP and 14.172–14.392 Å (14.262 Å on average) for LKC-UP; and 14.202–14.366 Å (14.275 Å on average) for the Orhanlar Unit. For the Çal Unit, the average reflection value is 14.269 Å.

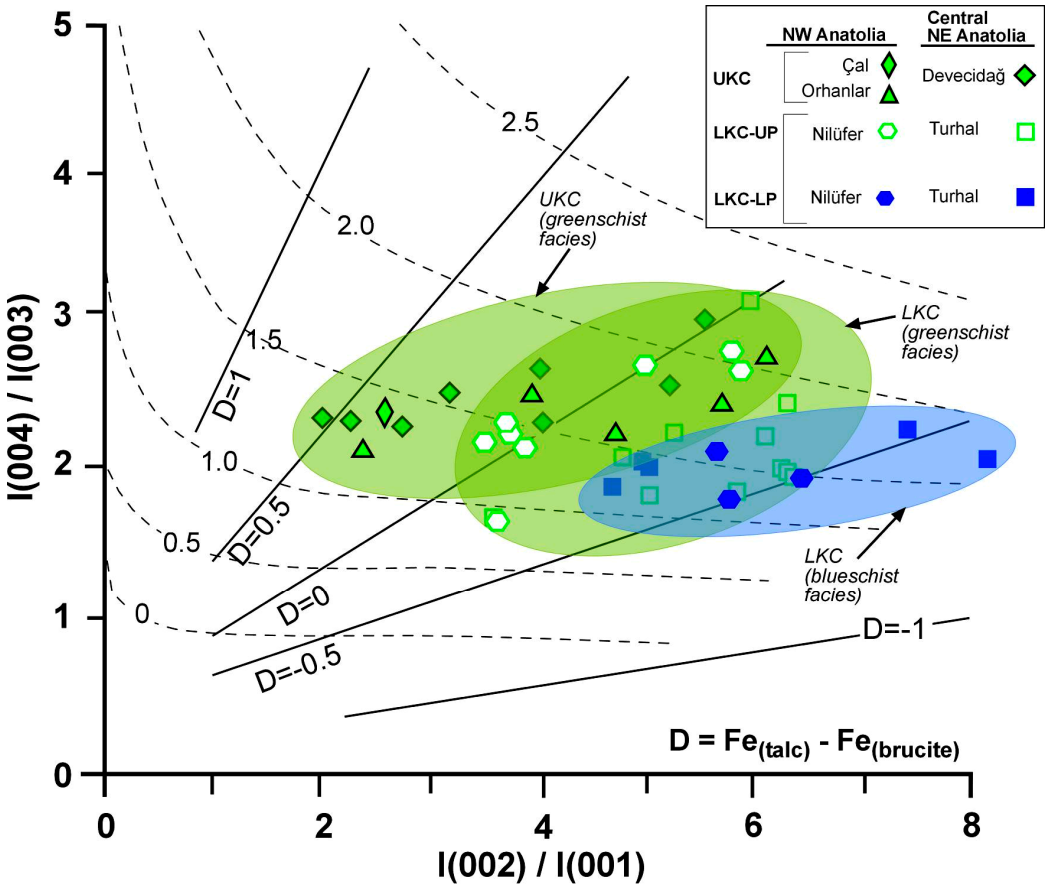

Figure 7. Fe content within the talc layer and distribution of talc and brucite layers of chlorite minerals according to basal peak ratios [44] in the Karakaya Complex units.

Table 3. X-ray diffraction (XRD) basal reflections and chemical compositions of chlorite minerals in the Lower Karakaya Complex units. B: Brindley [42], B&B: Brindley and Brown [43], C&D: Chagnon and Desjardins [44]), $Al^{IV} = Al^{VI}$ and $Mg = 6 - (Fe + Al^{IV})$.

Sample No.	$d_{(001)}$ (Å)	*I*(003)/ *I*(001)	*I*(002 + 004)/ *I*(001 + 003)	*I*(002)/ *I*(001)	*I*(004)/ *I*(003)	Talc Fe^{+2}		Brucite Fe^{+2}		Σ Fe^{+2}		Al^{IV}	Mg^{VI}	Fe/(Fe + Mg)
						B&B	C&D	B&B	C&D	B&B	C&D	B&B	C&D	C&D
NW Anatolia														
LKC-UP (Greenschist facies)														
NKK-95	14.231	1.26	4.05	5.89	2.59	1.87	1.98	2.58	2.13	4.45	4.11	1.10	0.79	0.84
-96	14.392	2.16	3.39	5.01	2.64	1.07	1.90	2.60	1.90	3.67	3.80	0.54	1.66	0.70
-97	14.172	1.36	4.02	5.79	2.71	1.79	2.10	2.61	2.20	4.40	4.30	1.30	0.40	0.92
-98	14.311	1.29	2.88	3.89	2.10	1.13	1.43	1.88	1.44	3.01	2.87	0.82	2.31	0.55
-103	14.280	1.98	2.72	3.77	2.19	0.69	1.48	2.09	1.40	2.78	2.88	0.93	2.19	0.57
-106	14.200	1.18	2.81	3.51	2.22	1.15	1.50	1.76	1.30	2.91	2.80	1.21	1.99	0.58
-108	14.287	1.13	2.98	3.70	2.34	1.30	1.60	1.84	1.40	3.14	3.00	0.91	2.09	0.59
-111	14.220	1.95	3.33	5.65	2.15	1.11	1.60	2.49	1.95	3.60	3.55	1.14	1.31	0.73
LKC-LP (Blueschist facies)														
-113	14.220	3.44	2.67	5.77	1.77	0.24	1.20	2.47	1.70	2.71	2.90	1.14	1.96	0.60
-115	14.189	2.53	3.23	6.43	1.97	0.85	1.50	2.62	2.00	3.47	3.50	1.24	1.26	0.74
-117	14.338	1.72	2.36	3.63	1.62	0.54	0.90	1.72	1.20	2.26	2.10	0.73	3.17	0.40
Central NE Anatolia														
LKC-UP (Greenschist facies)														
TKK-4	14.372	1.51	4.31	5.97	3.22	1.81	2.30	2.79	2.30	4.60	4.60	0.61	0.79	0.85
-10	14.192	3.56	3.81	9.27	2.28	1.11	1.90	3.39	2.60	4.50	4.50	1.23	0.27	0.94
-28	14.269	1.88	2.38	3.59	1.74	0.34	0.85	1.66	1.15	2.00	2.00	0.97	3.03	0.40
-49	14.231	1.94	2.97	5.03	1.90	0.79	1.27	2.15	1.67	2.94	2.94	1.10	1.96	0.60
-50	14.251	1.54	3.48	5.27	2.32	1.27	1.65	2.28	1.90	3.55	3.55	1.03	1.42	0.71
-58	14.251	2.85	3.28	6.11	2.29	0.83	1.65	2.77	1.95	3.60	3.60	1.03	1.37	0.72
-63	14.220	2.85	3.15	6.31	2.04	0.79	1.55	2.74	1.98	3.53	3.53	1.14	1.33	0.73
-64	14.182	2.22	3.37	6.25	2.07	0.97	1.55	2.53	1.95	3.52	3.50	1.27	1.23	0.74
-73	14.311	2.23	3.70	6.30	2.53	1.24	1.90	2.81	2.15	4.05	4.05	0.82	1.13	0.78
-82	14.259	1.76	3.11	4.78	2.16	1.02	1.50	2.23	1.75	3.25	3.25	1.00	1.75	0.65
-84	14.190	2.20	3.13	5.85	1.90	0.86	1.40	2.42	1.88	3.28	3.28	1.24	1.48	0.69
LKC-LP (Blueschist facies)														
-42	14.200	1.69	2.72	4.30	1.79	0.72	1.10	1.88	1.50	2.60	2.60	1.21	2.19	0.54
-36	14.200	1.67	2.32	3.45	1.64	0.53	1.00	1.67	1.20	2.20	2.20	1.21	2.59	0.46
-38	14.311	1.45	2.06	2.81	1.55	0.38	0.74	1.29	0.93	1.67	1.67	0.82	3.51	0.32
-54	14.220	2.09	2.45	4.29	1.57	0.30	0.80	1.78	1.28	2.08	2.08	1.14	2.78	0.43
-68	14.291	1.79	2.86	4.23	2.09	0.85	1.40	2.10	1.55	2.95	2.95	0.89	2.16	0.58
-79	14.239	1.71	3.43	5.43	2.27	0.75	1.65	1.92	2.02	2.67	2.67	1.07	2.26	0.54

Table 4. XRD basal reflections and chemical compositions of chlorite minerals in the Upper Karakaya Complex units (subgreenschist facies). B: Brindley [42], B&B: Brindley and Brown [43], C&D: Chagnon and Desjardins [44]), $Al^{IV} = Al^{VI}$ and $Mg = 6 - (Fe + Al^{IV})$.

Sample	$d_{(001)}$	$I(003)/$	$I(002 + 004)/$	$I(002)/$	$I(004)/$	Talc Fe^{2+}		Brucite Fe^{2+}		Σ Fe^{2+}		Al^{IV}	Mg^{VI}	Fe/(Fe + Mg)
No.	(Å)	$I(001$	$I(001 + 003)$	$I(001)$	$I(003)$	B&B	C&D	B&B	C&D	B&B	C&D	B&B	C&D	C&D
NW Anatolia														
CKK-163	14.269	0.71	2.49	2.58	2.35	1.30	1.42	1.15	1.02	2.45	2.44	0.98	2.58	0.48
BKK-188	14.366	1.38	3.11	3.96	2.49	1.23	1.65	2.08	1.50	3.31	3.25	0.63	2.12	0.61
-189	14.281	1.29	3.84	5.70	2.39	1.73	1.90	2.47	2.20	4.20	4.10	0.93	0.97	0.81
-190	14.220	1.50	3.22	4.72	2.22	1.24	1.55	2.22	1.70	3.46	3.25	1.14	2.61	0.46
-191	14.220	0.64	2.27	2.38	2.10	1.22	1.23	0.91	0.88	2.13	2.11	1.14	2.75	0.43
-193	14.287	1.40	4.12	6.11	2.69	1.82	2.15	2.69	2.35	4.51	4.50	0.91	0.59	0.88
Central NE Anatolia														
DKK-222	14.364	0.92	3.35	3.99	2.66	1.69	1.80	1.93	1.80	3.62	3.60	0.64	1.76	0.67
-223	14.130	1.23	3.09	4.04	2.31	1.30	1.65	1.98	1.60	3.28	3.25	1.45	1.30	0.71
-224	14.368	0.91	3.34	3.94	2.69	1.69	1.85	1.92	1.70	3.51	3.55	0.63	1.82	0.66
-225	14.269	0.55	2.28	2.27	2.29	1.35	1.35	0.79	0.90	2.24	2.25	0.97	2.78	0.45
-226	14.226	1.59	3.59	5.23	2.55	1.43	1.95	2.49	2.00	3.92	3.95	1.12	0.93	0.81
-234	14.216	0.95	2.84	3.18	2.48	1.33	1.60	1.62	1.30	2.95	2.90	1.15	1.95	0.60
-235	14.267	0.63	2.12	2.00	2.32	1.12	1.27	0.79	0.73	1.91	2.00	0.98	3.02	0.40
-243	14.262	1.21	4.15	5.55	2.99	1.95	2.25	2.60	2.20	4.45	4.45	0.99	0.56	0.89
-250	14.351	0.72	2.54	2.74	2.27	1.34	1.40	1.20	1.15	2.54	2.55	0.69	2.76	0.48

According to the methods outlined by Brindley and Brown [43] and Chagnon and Desjardins [44], the Fe content in talc and brucite layers of the chlorites are similar, and the Chagnon and Desjardins [44] method was taken as a basis for determining octahedral Fe (Figure 7). According to the diagram, the Fe contents in the talc layer of the chlorites range between 1.0 and 2.4. Therefore, 2.10–3.50 (2.83 on average) was established for the octahedral Fe contents of the chlorites for LKC-UP in NW Anatolia, 2.80–4.11 (3.41 on average) for LKC-UP, and 2.11–4.50 (3.44 on average) and 2.44 for UKC Orhanlar and Çal units, respectively. Octahedral Al contents are 0.73–1.24 (1.04 on average) for LKC-LP, 0.54–1.21 (0.99 on average) for LKC-UP, and 0.63–1.14 (0.94 on average) and 0.98 for UKC (Orhanlar and Çal units), respectively. Octahedral Mg contents are 1.26–3.17 (2.13 on average) for LKC-LP, 0.40–2.31 (1.59 on average) for LKC-UP, and 0.56–2.75 (1.62 on average) and 2.58 for UKC (Orhanlar and Çal units), respectively. Total amounts of octahedral cations for LKC-L, LKC-U and UKC (Orhanlar and Çal units) is 6.00 and it was noted that the chlorites are of trioctahedral component and the average structural formulae are provided below:

$$(Al_{0.94}Fe_{3.44}Mg_{1.62})[(Si_{3.06}Al_{0.94})O_{10}](OH)_8 \text{ (UKC Orhanlar)}$$

$$(Al_{0.98}Fe_{2.44}Mg_{2.58})[(Si_{3.02}Al_{0.98})O_{10}](OH)_8 \text{ (UKC Çal)}$$

$$(Al_{0.98}Fe_{3.47}Mg_{1.55})[(Si_{3.02}Al_{0.98})O_{10}](OH)_8 \text{ (LKC-UP)}$$

$$(Al_{1.00}Fe_{3.26}Mg_{1.74})[(Si_{3.00}Al_{1.00})O_{10}](OH)_8 \text{ (LKC-LP)}$$

$d_{(001)}$ values of the chlorites of Turhal Metamorphites LKC-LP, LKC-UP and UKC-Devecidağ Melange in the central NE Anatolia are 14.200–14.311 Å (14.244 Å on average), 14.190–14.372 (14.248 on average) and 14.130–14.368 Å (14.273 Å on average). Octahedral Fe contents are 1.67–2.95 (2.36 on average), 2.00–4.60 (3.53) and 2.00–4.45 (3.17 on average); octahedral Al contents are 0.82–1.21 (1.06 on average), 0.61–1.27 (1.04 on average) and 0.63–1.45 (0.96 on average). Octahedral Mg contents are 2.16–3.51 (2.58 on average), 0.27–1.96 (1.43 on average) and 0.56–3.02 (1.88 on average), respectively. Total octahedral cation amounts are 6.00 and it was determined that they are closer to trioctahedral composition. The overall average structural formulas of the chlorites are as follow:

$$(Al_{0.96}Fe_{3.16}Mg_{1.88})[(Si_{3.04}Al_{0.96})O_{10}](OH)_8 \text{ (UKC Devecidağ Melange)}$$

$$(Al_{1.04}Fe_{3.53}Mg_{1.43})[(Si_{2.96}Al_{1.04})O_{10}](OH)_8 \text{ (LKC-UP Turhal Metamorphites)}$$

$$(Al_{1.06}Fe_{2.36}Mg_{2.58})[(Si_{2.94}Al_{1.06})O_{10}](OH)_8 \text{ (LKC-LP Turhal Metamorphites)}$$

The substitution of Al in the place of tetrahedral Si leads to a reduction in layer thickness and thus a reduction in $d_{(001)}$ value as a result of the strengthening of the layer and the bond between the layers [45].

On the basis of the diagram using Al^{IV} − Fe/(Fe + Mg) ratios [46] the, LKC-LP chlorites examined here fall in brunsvigit-diabantite zone, whereas LKC-UP chlorites cluster in brunsvigit zone; UKC chlorites plot within the diabandite-chamosite zone and show variable compositions. According to the AIPEA classification [47], the chlorites investigated here classify mainly as chamosite and partly clinochlore compositions (Figure 8). In contrast, it is observed that only one (NKK-113) of the two samples defined as IIb polytype falls within the area defined by Foster [46].

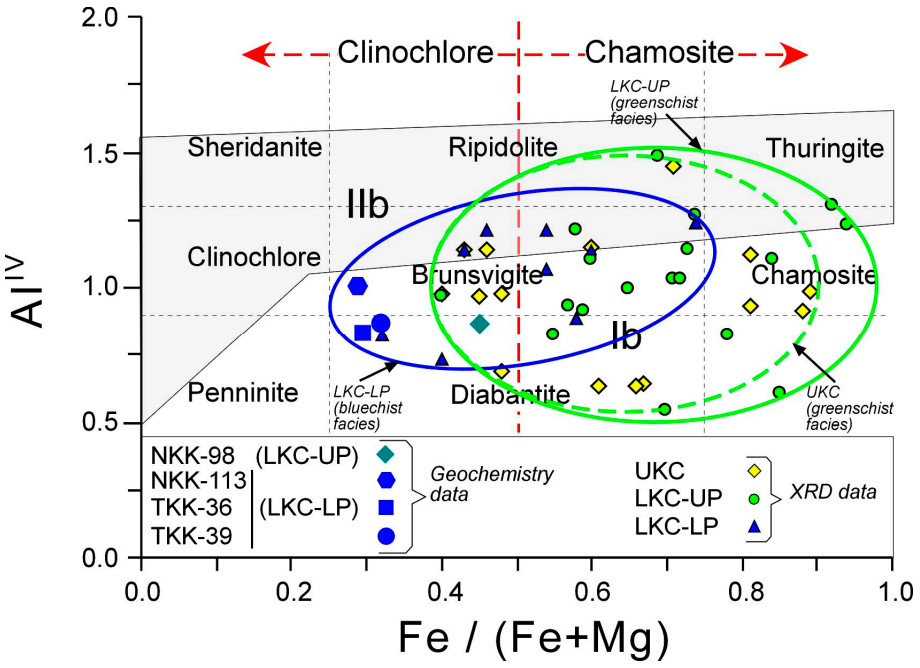

Figure 8. The setting of chlorite minerals in the Karakaya Complex units in tetrahedral Si-octahedral Fe/(Fe + Mg) diagram (Classification and IIb polytype area: Foster [46]; Ib polytype area: Curtis *et al.* [5]; chamosite-clinochlore boundary: Bailey [47]).

Distributions of the first three basal reflections (I_{001}, I_{002} and I_{003}) of the chlorites [16] indicate that the LKC and UKC units are distinct (Figure 9). The intensities of the chlorites shift in a way such that they get closer to the I_{002}-I_{003} line as their Fe/(Fe + Mg) contents increase. The difference in intensities for the LKC-UP and LKC-LP units relative to their I_{002} and I_{003} can be attributed to their relatively higher iron and magnesium contents, respectively. Moreover, the high intensities related to 003 peaks in LKC-LP are the result of higher Fe contents in brucite layers rather than talc layers (Figure 7).

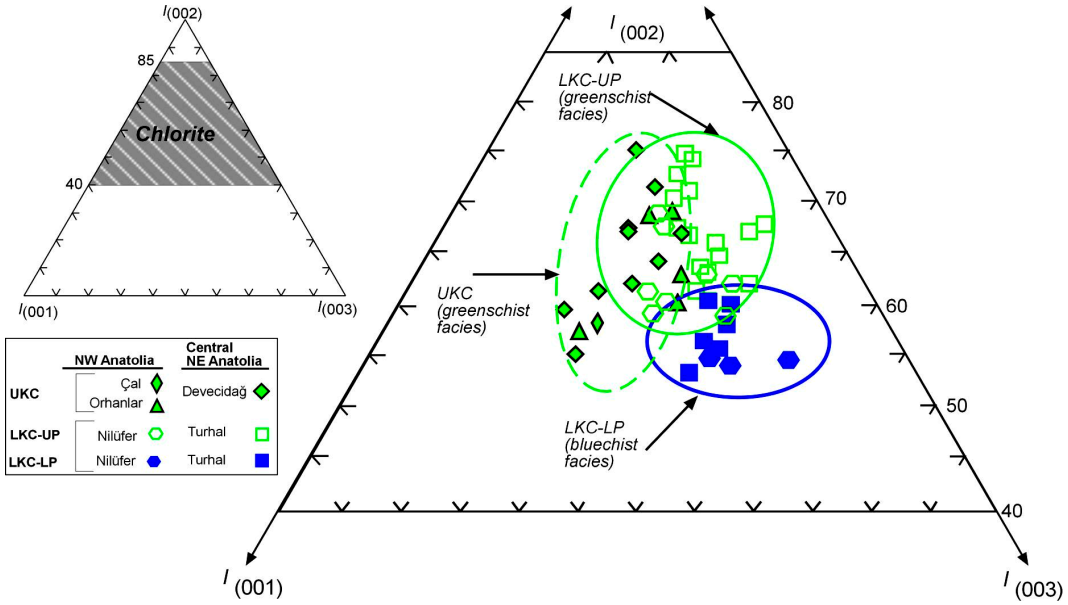

Figure 9. The distribution of chlorite minerals in the Karakaya Complex units in the triangular diagram according to the first three basal reflections (Chlorite area: Árkai and Ghabrial [16]).

4.2.4. Crystallinity

Arkai (AI: [15,36]) and Kübler Index values (KI: [35]) measured in the chlorite minerals of KC units are provided in Table 5. Accordingly, AI values of LKC-LP were detected as 0.23–0.28 Δ°2θ (0.26 Δ°2θ on average) and 0.14–0.31 (0.20 Δ°2θ on average) for NW and the central NE Anatolia, respectively. AI values for the chlorites representing LKC-UP were detected as 0.22–0.35 Δ°2θ (0.28 Δ°2θ on average) and 0.13–0.34 Δ°2θ (0.22 Δ°2θ on average) for NW and the central NE Anatolia regions respectively. All these values point to the anchizone near the border of anchizone-epizone and epizone area (AI < 0.26). KI values in LKC-LP illites were measured as 0.21 Δ°2θ only for the central NE Anatolia. KI values in LKC-UP illites were detected as 0.22–0.37 Δ°2θ (0.31 Δ°2θ on average) and 0.23–0.28 Δ°2θ (0.25 Δ°2θ on average) for NW and the central NE Anatolia, respectively. These values represent the epizone area (KI < 0.25) for LKC-LP and the anchizone area for LKC-UP.

As for UKC units, AI values for NW and the central NE Anatolia regions were measured as 0.37–0.56 Δ°2θ (0.46 Δ°2θ on average) and 0.27–0.39 Δ°2θ (0.31 Δ°2θ on average), respectively. Average values are distributed in anchizone (AI = 0.26–0.33 Δ°2θ) and diagenesis (AI > 0.33 Δ°2θ) areas. KI values in UKC units were found as 0.31–0.49 Δ°2θ (0.41 Δ°2θ on average) and 0.21–0.38 Δ°2θ (0.29 Δ°2θ on average) for NW and the central NE Anatolia regions respectively. Average values indicate the anchizone area.

Combined AI and KI data indicate that crystallinity decreases for samples from LKC units compared to the UKC units and the units diverge (Figure 10). There is a weak correlation relation between KI and AI values and it is different than (epizone: 0.21 Δ°2θ, anchizone: 0.53 Δ°2θ) the AI values corresponding to the epizone (AI < 0.26 Δ°2θ) and anchizone (AI = 0.26–0.37 Δ°2θ) as suggested by Árkai [15].

Table 5. Crystallinity index values of chlorite (AI) and illite (KI) in the Karakaya Complex units.

KC	Area	Unit	Sample No.	AI (001)	KI (001)	Area	Unit	Sample No.	AI (001)	KI (001)	Sample No.	AI (001)	KI (001)
UKC	NW Anatolia	Çal	CKK-163	0.36	0.49	Central NE Anatolia	Devecidağ	DKK-222	0.32	0.21	-234	0.30	0.25
		Orhanlar	BKK-188	0.37	0.41			-223	0.30	0.29	-235	0.30	0.26
			-197	0.56	0.31			-224	0.33	0.35	-243	0.31	0.38
			-199	0.40	0.41			-225	0.31	0.31	-245	0.29	0.31
			-	-	-			-226	0.27	0.29	-250	0.39	-
LKC-UP		Nilüfer	NKK-95	0.22	0.22		Turhal Metamorphites	TKK-4	0.13	0.26	-51	0.26	0.27
			-96	0.25	-			-10	0.15	-	-58	0.14	-
			-97	0.28	0.29			-11	0.22	0.23	-63	0.34	-
			-98	0.24	-			-25	0.22	-	-64	0.26	-
			-103	0.31	-			-28	0.15	-	-65	0.25	0.30
			-106	0.33	0.34			-30	0.24	0.26	-73	0.24	-
			-108	0.35	0.37			-31	0.19	0.15	-82	0.27	-
			-111	0.27	-			-49	0.20	0.23	-84	0.30	-
			-	-	-			-50	0.21	0.27	-	-	-
LKC-LP			-113	0.23	-			-36	0.16	-	-54	0.15	-
			-115	0.26	-			-38	0.31	-	-68	0.24	-
			-117	0.28	-			-42	0.22	0.21	-79	0.14	-

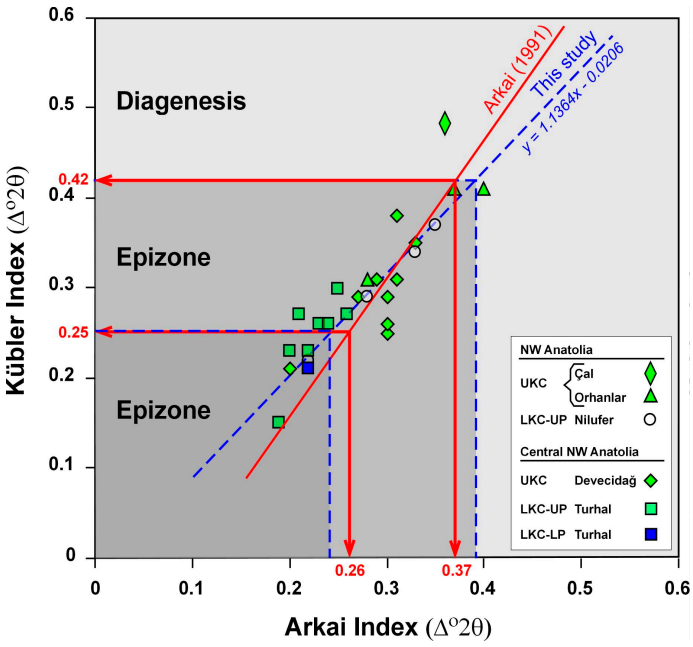

Figure 10. Relationships between Kübler Index (Δ°2θ)-Arkai Index (Δ°2θ) in the Karakaya Complex units (red line and values: Arkai [15]).

4.3. Geochemistry

Structural formulas [48] of the chlorite minerals for the KC units were calculated based on the major and trace element contents and 14 oxygen atoms (per formula unit) and are listed in Tables 6 and 7. The structural formulas of two samples were recalculated by removing Al_2O_3 and SiO_2 percentages depending on K_2O, Na_2O and CaO with 1:1:6 and 1:1:2 ratios of theoretical feldspar composition (K-feldspar $K_2O \cdot Al_2O_3 \cdot 6SiO_2$, albite $Na_2O \cdot Al_2O_3 \cdot 6SiO_2$, anortite $CaO \cdot Al_2O_3 \cdot 2SiO_2$) in the clay fraction. The charge deficiency resulting from the introduction of Al from feldspar within chlorite is balanced by K, Na, and Ca from the feldspars.

Table 6. Major element composition and structural formulas of chlorite minerals in the Karakaya Complex units (*: The values show that theoretical feldspar composition is removed, $\sum Fe_2O_3$: Total iron as Fe_2O_3, LOI: Loss on ignition at 1000 °C, TC: Tetrahedral charge, TOC: Total octahedral charge, OC: Octahedral charge, ILC: Interlayer charge, TLC: Total layer charge).

Area	**NW Anatolia**			**Central NE Anatolia**		
Unit	**LKC-UP**		**LKC-LP**	**LKC-LP**	**LKC-LP**	
Rock	**Metatuffite**		**Slate**	**Metatuffite**	**Schist**	
% Weigth	**NKK-98***		**NKK-113**	**TKK-36**	**TKK-39***	
SiO_2	51.73	32.07	31.45	32.98	44.03	32.43
TiO_2	0.470	0.882	2.355	0.717	1.111	1.54
Al_2O_3	17.74	18.32	15.95	15.71	11.35	11.44
ΣFe_2O_3	11.22	21.06	16.49	17.21	15.05	20.80
MnO	0.157	0.295	0.377	0.160	0.192	0.27
MgO	6.90	12.95	20.49	20.76	16.31	22.54
CaO	0.60	1.13	1.84	0.10	2.27	0.01
Na_2O	3.78	0.02	0.70	0.04	1.93	0.01
K_2O	0.77	0.02	0.06	0.05	0.12	0.03
P_2O_5	0.21	0.39	0.06	0.03	0.03	0.04
LOI	6.85	12.86	9.98	10.89	7.89	10.90
Total	100.73	100.00	99.75	98.65	100.28	100.00
Si	-	3.13	3.00	3.17	-	3.13
Al	-	0.87	1.00	0.83	-	0.87
TC	-	0.87	1.00	0.83	-	0.87
Ti	-	0.06	0.17	0.05	-	0.11
Al	-	1.24	0.79	0.95	-	0.87
Fe	-	1.55	1.18	1.25	-	1.51
Mn	-	0.02	0.03	0.01	-	0.02
Mg	-	1.89	2.91	2.98	-	3.25
TOC	-	4.77	5.08	5.24	-	5.33
OC	-	0.46	0.47	0.78	-	0.84
Ca	-	0.12	0.19	0.01	-	0.00
Na	-	0.00	0.13	0.01	-	0.00
K	-	0.00	0.01	0.01	-	0.00
P	-	0.03	0.00	0.00	-	0.00
ILC	-	0.40	0.54	0.05	-	0.00
TLC	-	0.40	0.54	0.05	-	0.03

Tetrahedral Si-Al (1.00–0.83) and octahedral Mg-Fe-Al (4.64–4.79) substitutions yield total calculated octahedral cations in excess of 4 (4.77–5.33) in samples of chlorite from slate of the Nilüfer unit and the metatuffite of Turhal Metamorphites, which indicate their di-trioctahedral composition and is verified by the XRD data.

Chlorites plot within the Type I zone represented by Mg-Fe chlorites (trioctahedral) in Al + □ − Mg − Fe diagram [49]. According to the Zane and Weiss [49] classification, the source for the LKC-LP chlorites generally correspond to metabasic rocks, whereas those for the LKC-UP chlorites are felsic rocks, and those for the UKC chlorites correspond to both felsic and metabasic sources, with felsic being predominant (Figure 11).

The trace element concentrations of chlorite minerals are compared in Figure 12, and these are extremely variable. The substitution of elements with similar geochemical behaviour is mostly observed in the metatuff sample of Nilüfer unit. The highest trace element enrichment for the chlorites is observed in the LKC-LP unit (TKK-36) and the lowest in the LKC-UP unit (NKK-98). Cr, Ni, V, and Cu (transition elements), Ga (low field strength elements-LFSEs), and Nb, Zr and U (high field strength elements-HFSEs) record the highest enrichment in LKC-LP chlorites. As for LKC-UP chlorites, Zn (transition elements), W (lithophile elements); and Rb, Ba and Sr (LFSEs) are present at high concentrations. Hence, trace element concentrations are a function of the protoliths, *i.e.*, igneous *versus* metamorphic parent materials.

Chondrite-normalized trace element patterns for chlorite are shown in Figure 13. Trace element concentrations for the North American Shale Composite (NASC) are from Gromet *et al.* [50], with the exception of Nb and Y (from Condie, [51]). The chlorite minerals exhibit marked variation when compared to chondrite values, and generally have lower concentrations relative to NASC, except for Ti and U. The latter shows an enrichment of up to 5600 times in the volcanogenic chlorite for sample LKC-LP (TKK-36) and therefore exhibits a strong positive anomaly (Figure 13). In all chlorites, K, Sr, and P display significant negative anomalies. The chlorite from sample TKK-30 within the LKC-LP exhibits the lowest chondrite normalized values.

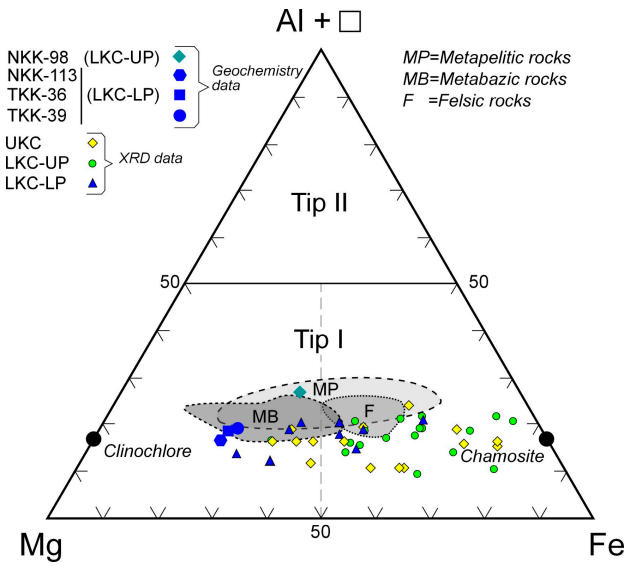

Figure 11. The distribution of chlorites in the Karakaya Complex units in the Al+ □ − Mg − Fe triangular diagram according to octahedral compositions (□: Octahedral vacancy).

Table 7. Trace element composition of chlorite minerals in the Karakaya Complex units (<: Concentrations are below the detection limit).

Area	NW Aantolia		Central NE Anatolia	
Unit	LKC-UP	LKC-LP	LKC-LP	LKC-LP
Rock	Metatuffite	Slate	Metatuffite	Schist
ppm	NKK-98	NKK-113	TKK-36	TKK-39
Cr	270	440	1330	850
Ni	130	230	890	400
Co	23	73	102	62
Sc	29	10	24	24
V	214	231	327	226
Cu	40	280	160	90
Pb	11	<5	34	<5
Zn	290	230	160	130
Bi	<0.1	1.0	0.7	<0.1
In	<0.1	<0.1	<0.1	<0.1
Sn	2	3	<1	<1
W	72.6	3.4	20.8	16.4
Mo	<2	<2	<2	3
As	21	<5	19	5
Sb	11.1	0.7	7.1	0.3
Ge	2.3	0.5	2.0	2.1
Be	2	2	3	<1
Ag	1.0	<0.5	<0.5	0.8
Rb	32	1	6	3
Cs	2.3	<0.1	0.4	2.1
Ba	174	17	14	7
Sr	172	8	6	14
Tl	0.24	<0.05	<0.05	<0.05
Ga	26	33	26	20
Ta	0.63	1.24	1.02	0.56
Nb	3.1	21.8	10.9	6.3
Hf	3.7	5.3	1.5	2.6
Zr	139	204	71	104
Y	27.4	22.9	7.0	12.3
Th	11.2	1.19	1.13	1.22
U	3.70	0.55	44.8	0.34
La	27.6	2.04	4.42	8.81
Ce	60.0	6.2	9.0	18.9
Pr	6.56	0.83	0.96	2.20
Nd	24.70	5.55	3.85	9.28
Sm	4.84	2.30	0.93	2.19
Eu	1.190	0.863	0.331	0.796
Gd	4.00	3.38	1.12	2.18
Tb	0.71	0.67	0.20	0.38
Dy	4.42	4.31	1.27	2.34
Ho	0.94	0.85	0.24	0.46
Er	2.96	2.39	0.66	1.23
Tm	0.462	0.345	0.087	0.175
Yb	3.11	2.09	0.49	1.12
Lu	0.510	0.314	0.066	0.186

The chlorite chondrite normalized REE abundances are shown in Figure 14. NASC values (with the exception of Ho and Tm; Haskin *et al.* [52]) are taken from Gromet *et al.* [50]. REE contents of all chlorite minerals are lower than NASC and exhibit varying degrees of enrichment compared to chondrite [53]. The highest chondrite normalized values are displayed by the volcanogenic chlorite (NKK-98) from the LKC-UP unit, whereas the lowest values are recorded in the volcanogenic chlorite (TKK-36) from the LKC-LP unit. Furthermore, light REE (LREEs; La-Gd) concentrations of chlorite minerals show a slight decrease when compared to those for the heavy REEs (HREEs; Tb-Lu). In the chlorite for the LKC-LP unit within the NW-Anatolia, Pr defines a negative anomaly, while Sm yields a slight positive anomaly.

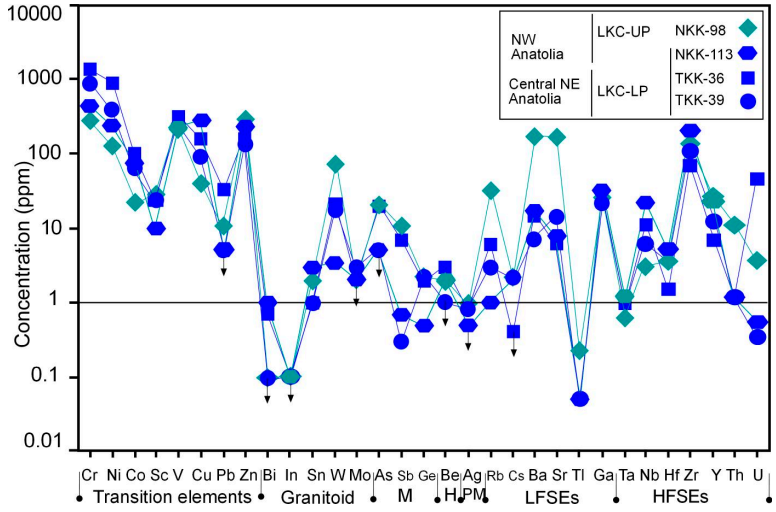

Figure 12. The correlation of chlorite minerals in the Karakaya Complex units according to the contents of trace elements (Arrows show values below the detection limits, M = Miscellaneous elements, H = Halogen elements, PM = Precious metals, LFSEs = Low field strength elements, HFSEs = High field strength elements).

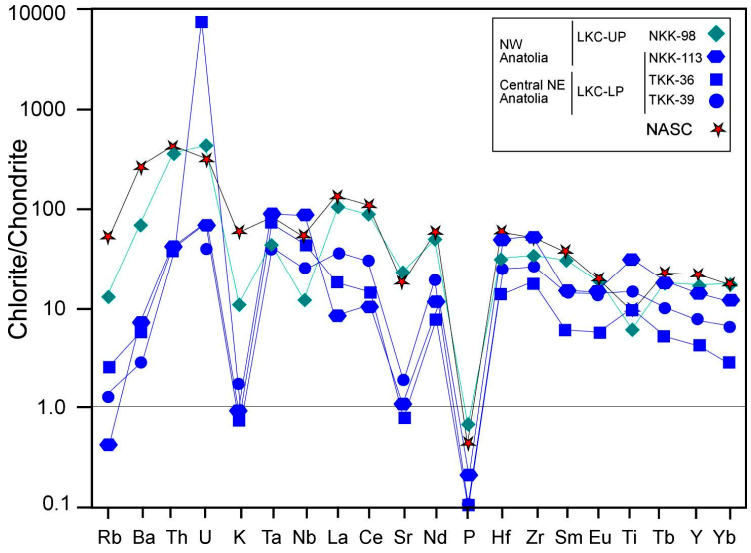

Figure 13. Chondrite-normalized trace element pattern of chlorite minerals in the Karakaya Complex units (Chondrite: Sun and Mcdonough [53]; Nb and Y for North American Shale Composite (NASC): [51]; other elements: Gromet *et al.* [50]).

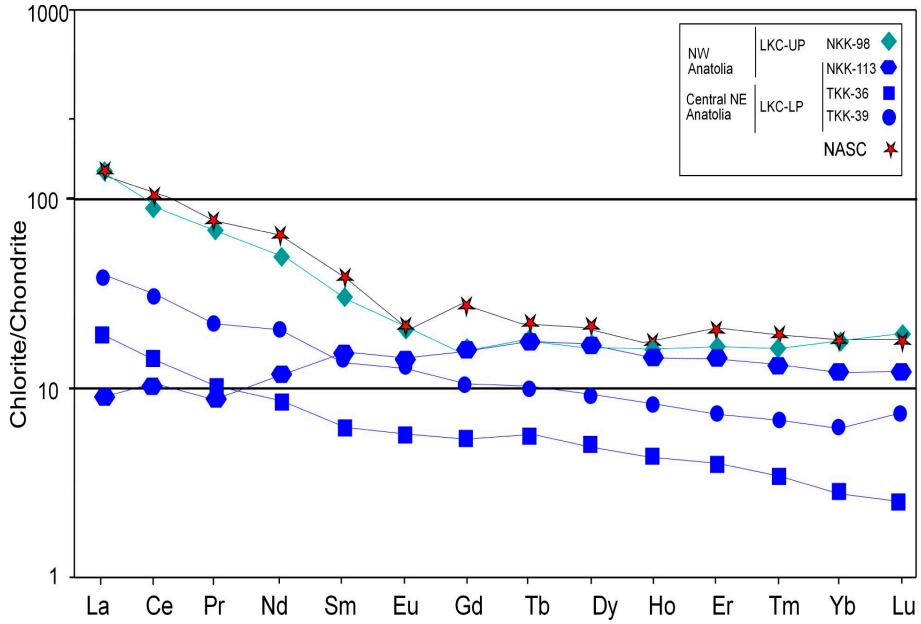

Figure 14. Chondrite-normalized rare earth element (REE) pattern of chlorite minerals in the Karakaya Complex units (Ho and Tm for NASC: Haskin *et al.* [52], other elements: Gromet *et al.* [50]; Chondrite: Sun and McDonough [53]).

5. Conclusions

Chlorite within the units of the Karakaya Complex representing NW and NE Anatolia are of neoformed origin in the groundmass and/or matrix and pores, and display different optical properties and morphologies. It is proposed that volcanic glass and/or matrix-chlorite transformation occurs via a permeating aqueous MgFeAl-silicate gel intermediate phase (Volcanic glass and/or matrix + Ions → Aqueous MgFeAl-silicate gel → Chlorite + Water: Yalçın *et al.* [54]):

$$7SiO_2 \cdot Al_2O_3 \cdot 2MgO \cdot 2FeO + 24OH^- + 10H^+ \rightarrow 9MgO \cdot 2FeO \cdot 2Al(OH)_3 \cdot 7Si(OH)_4 \rightarrow Mg_9Fe_2Al[AlSi_7O_{20}](OH)_{16} + 9H_2O$$

The Mg content of chlorite is higher in the LKC-LP blueschist facies, while the Fe content in the LKC-UP greenschist is related to the mineralogical composition of the rocks as a result of the increasing heat/pressure due to burial depth. The difference in metamorphic degree, in particular between the LKC-LP (blueschist) and LKC-UP (greenschist) units, seems to have also affected the chemical compositions of the chlorites since the latter can be related to lithological differences and the nature of the protolith.

The 7 Å (Δ°2θ) peak width for chlorite was examined by several previous studies [15,55–62], and these indicate that chlorite crystallinity is more apparent compared to that for illite, in particular for basic-metabasic rocks [15,58,60,62]. As the grade of diagenesis/metamorphism increases, chlorite crystallinity also increases as is the case for illite/muscovite. In the samples investigated here, AI values correspond to those for the epizone-anchizone for LKC units, whereas those for the UKC units are consistent with low-degree anchimetamorphic-diagenetic stage. For units within NW and the central NE Anatolia, illite crystallinity (Kübler Index: Kübler [35]) seems to be compatible with AI values [19–21].

The features of transition to semi-regular or regular stacking are observed in chlorite layers [47,63,64], and these structural (polytype) changes may be partly attributed to heating, which then serves as a qualitative method for geothermometric assessment [65]. It has been established that the transformation from Ib → IIb type chlorites occurs at temperatures <200 °C [10]; the chlorites investigated here are IIb and those for Turhal Metamorphites within the UKC units are of $2M_1$ polytype [20], both of which indicate a similar degree of metamorphism.

The combined optical, mineralogical, morphological, and geochemical evidence reported here for chlorite are shown to be related to the structures, formation mechanisms, and tectonic environments present during their formation. Consequently, chlorite plays a key role in distinguishing units with distinct geological evolutions within the Karakaya Complex.

Acknowledgments

The authors extend their thanks for their help to Cumhuriyet University Directorate of Scientific Research Projects Commission (Project No: M 301) that gave financial support for the realization of this study, the deceased Mehmet DURU (General Directorate of Mineral Research and Exploration) and Ahmet GÖKÇE (Cumhuriyet University) who ensured the introduction of the units in NW Anatolia and the central NE Anatolia in the field respectively, Cumhuriyet University Department of Geology Engineering laboratory workers in XRD works and the preparation of thin sections and to TPAO workers for SEM examinations. In addition, M. Cemal GÖNCÜOĞLU has contributed to the shaping of the article with his suggestions and criticisms on the understanding of the geological evolution of the Karakaya Complex. We are also grateful to the academic editor and anonymous referees for their constructive comments leading to important improvements in the manuscript.

Author Contributions

Sema Tetiker was in charge of sampling, field analysis, interpretations, and scientific writing of this study under the supervision of Hüseyin Yalçın and Ömer Bozkaya.

Conflicts of Interest

The authors declare no conflict of interest.

References

1. Millot, G. *Geology of Clays*; Farrand, W.R., Paquet, H., Eds.; Springer Verlag: Berlin, Germany, 1970; p. 429.
2. Weaver, C.E.; Highsmith, P.B.; Wampler, J.M. Chlorite. In *Shale-Slate Metamorphism in the Southern Appalachians*; Weaver, C.E., Ed.; Elsevier: Amsterdam, The Netherlands, 1984; Volume 10, pp. 99–139.
3. Ahn, J.; Peacor, D.R. Transmission electron microscopic study of diagenetic chlorite in Gulf Coast argillaceous sediments. *Clays Clay Miner.* **1985**, *33*, 228–236.
4. Cathelineau, M.; Nieva, D. A chlorite solid solution geothermometer, the Los Azufres geothermal system (Mexico). *Contrib. Mineral. Petrol.* **1985**, *91*, 235–244.

5. Curtis, C.D.; Hughes, C.R.; Whiteman, J.A.; Whittle, C.K. Compositional variations within some sedimentary chlorites and some comments on their origin. *Mineral. Mag.* **1985**, *49*, 375–386.
6. Cathelineau, M. Cation site occupancy in chlorites and illites as a function of temperature. *Clay Miner.* **1988**, *23*, 471–485.
7. Velde, B.; Medhioub, M. Approach to chemical equilibrium in diagenetic chlorites. *Contrib. Mineral. Petrol.* **1988**, *98*, 122–127.
8. Jahren, J.S.; Aagard, P. Diagenetic illite-chlorite assemblages in arenites. I. Chemical evolution. *Clays Clay Miner.* **1992**, *40*, 540–546.
9. Hillier, S.; Velde, B. Octahedral occupancy and the chemical composition of diagenetic (low temperature) chlorites. *Clay Miner.* **1991**, *26*, 149–168.
10. Walker, J.R. Chlorite polytype geothermometry. *Clays Clay Miner.* **1993**, *41*, 260–267.
11. Xie, X.G.; Byerly, G.R.; Ferrell, R.E. IIb trioctahedral chlorite from the Barberton greenstone belt: Crystal structure and rock composition constraints with implications to geothermometry. *Contrib. Mineral. Petrol*. **1997**, *126*, 275–291.
12. Bozkaya, Ö.; Yalçın, H. Relationships between degree of diagenesis-metamorphism and chemistry of phillosilicates from eastern Taurus Aotochtonous. In Proceedings of the IXth Turkish National Clay Symposium, İstanbul, Turkey, 15–18 September 1999; pp. 21–30. (In Turkish).
13. Bozkaya, Ö.; Yalçın, H.; Schroeder, P.A.; Crowe, D. New insights in the definition of phyllosilicate stacks in diagenetic-metamorphic environments-examples from clastic to metaclastic rocks in Turkey. In Proceedings of the MECC14 7th Mid-European Clay Conference, Dresden, Germany, 16–19 September 2014; p. 117.
14. Árkai, P. Chlorite crystallinity: An empirical approach and correlation with illite crystallinity, coal rank and mineral facies as exemplified by Palaeozoic and Mesozoic rocks of northeast Hungary. *J. Metamorph. Geol.* **1991**, *9*, 723–734.
15. Árkai, P.; Tóth, M. Illite and chlorite "crystallinity" indices, I: An attempted mineralogical interpretation. In Proceedings of the IGCP Conference on Phyllosilicates as indicators of very low-grade metamorphism and diagenesis (IGCP 294), Manchester, UK, 4–6 July 1990.
16. Árkai, P.; Ghabrial, D.S. Chlorite crstallinity as an indicator of metamorphic grade of low-temperature meta-igneous rocks: A case study form the Bükk Mountains, Northeast Hungary. *Clay Miner.* **1997**, *32*, 205–222.
17. Árkai, P.; Sassi, F.P.; Sassi, R. Simultaneous measurements of chlorite and illite crystallinity: A more reliable geothermometric tool for monitoring low- to very low-grade metamorphisms in metapelites. A case study from the Southern Alps (NE Italy). *Eur. J. Mineral.* **1995**, *7*, 1115–1128.
18. Potel, S.; Ferreiro Mählmann, R.; Stern, W.B.; Mullis, J.; Frey, M. Very low-grade metamorphic evolution of pelitic rocks under high-pressure/low-temperature condition, NW New Caledonia (SW Pacific). *J. Petrol.* **2006**, *47*, 991–1015.
19. Tetiker, S.; Yalçın, H.; Bozkaya, Ö. Diagenesis-low grade metamorphism of Karakaya Complex units in the NW Anatolia. Hacettepe University. *Earth Sci. J.* **2009**, *30*, 193–212. (In Turkish)
20. Tetiker, S.; Yalçın, H.; Bozkaya, Ö. Low grade metamorphism of the units from Karakaya Complex (Tokat region). In Proceedings of the 14th Turkish National Clay Symposium, Trabzon, Turkey, 1–3 October 2009; pp. 155–173. (In Turkish)

21. Tetiker, S.; Yalçın, H.; Bozkaya, Ö.; Göncüoğlu, M.C. Diagenetic to low-grade metamorphic evolution of the Karakaya Complex in northern Turkey based on phyllosilicate mineralogy. *Mineral. Petrol.* **2015**, *109*, 201–215.
22. Şengör, A.M.C.; Yılmaz, Y.; Sungurlu, O. Tectonics of the Mediterranean Cimmerides: Nature and evolution of the western termination of Paleo-Tethys. In *The Geological Evolution of the Eastern Mediterranean*; Dixon, J.E., Robertson, A.H.F., Eds.; Special Publications Volume 17; Geological Society London: London, UK, 1984; pp. 77–112.
23. Göncüoğlu, M.C.; Dirik, K.; Kozlu, H. General chracteristics of pre-Alpine and Alpine Terranes in Turkey: Explanatory notes to the terrane map of Turkey. *Ann. Geol. Pays Hell.* **1997**, *37*, 515–536.
24. Okay, A.İ.; Göncüoğlu, M.C. The Karakaya Complex: A review of data and concepts. *Turk. J. Earth Sci.* **2004**, *13*, 77–95.
25. Robertson, A.H.F.; Ustaömer, T. Testing alternative tectono-stratigraphic interpretations of the Late Palaeozoic-Early Mesozoic Karakaya Complex in NW Turkey: Support for an accretionary origin related to northward subduction of Palaeotethys. *Turk. J. Earth Sci.* **2012**, *21*, 961–1007.
26. Tekeli, O. Subduction complex of pre-Jurassic age, Northern Anatolia, Turkey. *Geology* **1981**, *9*, 68–72.
27. Özcan, A.; Erkan, A.; Keskin, A.; Keskin, E.; Oral, A.; Özer, S.; Sümergen, M.; Tekeli, O. *Kuzey Anadolu Fayı Ile Kirşehir Masifi Arasının Temel Jeolojisi*; Appendix: Geological Map and Sections; Unpublished Report No: 6722; Institute of Mineral Research and Exploration: Ankara, Turkey, 1980; p. 136. (In Turkish)
28. Gökçe, A. Turhal Antimon Yataklarının Maden Jeolojisi. In *Doktora Tezi, Hacettepe Üniversitesi Jeoloji Mühendisliği Bölümü*; Fen Bilimleri: Ankara, Turkey, 1983; p. 150. (In Turkish)
29. Bailey, S.W.; McCallien, W.J. The Ankara melange and the Anatolian Thrust. *Nature* **1950**, *166*, 938–941.
30. Bailey, S.W.; McCallien, W.J. Serpentinite lavas, the Ankara melange and the Anatolian Thrust. *Trans. R. Soc. Edinb.* **1953**, *62*, 403–442.
31. Erol, O. Ankara Güneydoğusundaki Elma Dağı ve Çevresinin Jeolojisi ve Jeomorfolojisi Üzerine bir Araştırma. In *Bulletin of the Mineral Research and Exploration*; Institute of Mineral Research and Exploration: Ankara, Turkey, 1956; p. 99. (In Turkish)
32. Maden Tetkik ve Arama. Geologic Map of Turkey with the 1:500 000 scale, Istanbul Section. *General Directorate of Mineral Research and Exploration*; Institute of Mineral Research and Exploration: Ankara, Turkey, 2002. (In Turkish)
33. Brindley, G.W. Quantitative X-ray mineral analysis of clays. In *Crystal Structures of Clay Minerals and Their X-Ray Identification*; Brindley, G.W., Brown, G., Eds.; Mineralogical Society: London, UK, 1980; pp. 125–195.
34. Moore, D.M.; Reynolds, R.C., Jr. *X-Ray Diffraction and the Identification and Analysis of Clay Minerals*; Oxford University Press: New York, NY, USA, **1990**; p. 332.
35. Kübler, B. Evaluation quantitative du métamorphisme par la cristallinité de l'illite. *Bull. Cent. Rech. Pau-SNPA* **1968**, *2*, 385–397. (In French)

36. Guggenheim, S.; Bain, D.C.; Bergaya, F.; Brigatti, M.F.; Drits, A.; Eberl, D.D.; Formoso, M.L.L.; Galan, E.; Merriman, R.J.; Peacor, D.R.; *et al*. Report of the AIPEA nomenclature committee for 2001: Order, disorder and crystallinity in phyllosilicates and the use of the "Crystallinity Index". *Clay Miner.* **2002**, *37*, 389–393.
37. Kisch, H.J. Illite crystallinity and coal rank associated with lowest-grade metamorphism of the Taveyanne greywacke in the Helvetic zone of the Swiss Alps. *Eclogae Geol. Helv.* **1980**, *73*, 753–777.
38. Warr, L.N.; Rice, A.H.N. Interlaboratory standartization and calibration of clay mineral crystallinity and crystallite size data. *J. Metamorph.Geol.* **1994**, *12*, 141–152.
39. Krumm, S. WINFIT 1.2: Version of November 1996 (The Erlangen Geological and Mineralogical Software Collection) of WINFIT 1.0: A Public Domain Program for Interactive Profile-Analysis under Windows. In Proceedings of the XIII Conference on Clay Mineralogy and Petrology, Praha, Czech Republic, 29 August–2 September 1994; Volume 38, pp. 253–261.
40. Kisch, H.J. Calibration of the anchizone: A critical comparison of illite "crystallinity" scales used for definition. *J. Metamorph. Geol.* **1990**, *8*, 31–46.
41. Bailey, S.W. X-ray diffraction identification of the polytypes of mica, serpentine, and chlorite. *Clays Clay Miner.* **1988**, *36*, 193–213.
42. Brindley, G.W. Chlorite Minerals. In *The X-Ray Identification and Crystal Structures of Clay Minerals*; Brown, G., Ed.; Mineralogical Society: London, UK, 1961; pp. 242–296.
43. Brindley, G.W.; Brown, G. X-ray Diffraction Procedures for Clay Mineral Identification. In *Crystal Structures of Clay Minerals and Their X-ray Identification*; Brindley, G.W., Brown, G., Eds.; Mineralogical Society: London, UK, 1980; pp. 305–360.
44. Chagnon, A.; Desjardins, M. Determination de la composition de la chlorite par difraction et microanalyse aux rayons X. *Can. Mineral.* **1991**, *29*, 245–254. (In French)
45. Shirozu, H. X-ray powder patterns and cell dimensions of some chlorites in Japan with a note on their interference colors. *Mineral. J.* **1958**, *2*, 209–223.
46. Foster, M.D. Interpretation of the composition and a classification of the chlorites. *US Geol. Surv. Prof. Pap.* **1962**, *414*, 1–33.
47. Bailey, S.W. Summary of recommendations of AIPEA nomenclature committee on clay minerals. *Am. Mineral.* **1980**, *65*, 1–7.
48. Weaver, C.E.; Pollard, L.D. The Chemistry of Clay Minerals. In *Developments in Sedimentology*; Elsevier: Amsterdam, The Netherlands, 1973; Volume 15, p. 272.
49. Zane, A.; Weiss, Z. A procedure for classification of rock-forming chlorites based on microprobe data. *Rend. Fis. Accad. Lincei* **1998**, *9*, 51–56.
50. Gromet, L.P.; Dymek, R.F.; Haskin, L.A.; Korotev, R.L. The "North American shale composite": Its compilation, major and trace element characteristics. *Geochim. Cosmochim. Acta* **1984**, *48*, 2469–2482.
51. Condie, K.C. Chemical composition and evolution of the upper continental crust: Contrasting results from surface samples and shales. *Chem.Geol.* **1993**, *104*, 1–37.
52. Haskin, L.A.; Haskin, M.A.; Frey, F.A.; Wildeman, T.R. Relative and absolute terrestrial abundances of the rare earths. In *Origin and Distribution of the Elements*; Ahrens, L.H., Ed.; Pergamon Press: Oxford, UK, 1968; pp. 889–912.

53. Sun, S.S.; McDonough, W.F. Chemical and Isotopic Systematics of Oceanic Basalts: Implications for Mantle Composition and Processes. In *Magmatism in the Ocean Basins*; Saunders, A.D., Norry, M.J., Eds.; Geological Society London: London, UK, 1989; Special Publications Volume 42; pp. 313–345.
54. Yalçın, H.; Bozkaya, Ö.; Tetiker, S. Clay mineralogy and geochemistry of Kangal coal deposit. In Proceedings of the XIIth Turkish National Clay Symposium, Yüzüncü Yıl University, Van, Turkey, 5–9 September 2005; pp. 16–31. (In Turkish)
55. Ludwig, V. Zum übergang eines tonschiefers in die metamorphose: "Grieffelschiefer" des Ordoviziums in NE-Bayren (mit einem beitrag zum problem der illit-kristallinität). *Neues Jahrb. Geol. Paläontol. Abh.* **1973**, *144*, 50–103. (In German)
56. Schamel, S. Eocene Subduction in Central Liguria, Italy. Unpublished Ph.D. Thesis, Yale University, New Haven, CT, USA, 1973.
57. Le Corre, C. Analyse comparée de la cristallinité des micas dans le Briovérien et le Paléozoique Centre-Armoricains: Zonéographie et structure d'un domaine épizonal. *Bull. Soc. Géol. Fr.* **1975**, *17*, 547–553. (In French)
58. Schaer, J.P.; Persoz, F. Aspects strutcruaox et petrographtqoes du Hant Atlas calcaire de Midelt (Maroc). *Bull. Soc. Géol. Fr.* **1976**, *18*, 1239–1250. (In French)
59. Deutloff, O.; Teichmüller, M.; Teichmüller, R.; Wolf, M. Inkohlungs-untersuchungen im Mesozoikum des Massivs von Vlotho (Niedersädhsisches Tektogen). *Neues Jahrb. Geol. Paläontol. Monatsh.* **1980**, *6*, 321–341. (In German)
60. Dandois, P. Diagenèse et métamorphisme des domaines Calédonien et Hercynien de la vallée de la Meuse entre Charleville-Mezières et Namur (Ardennes franco-belges). *Ann. Soc. Géol. Belg.* **1981**, *90*, 299–316. (In French)
61. Duba, D.; Williams-Jones, A.E. The application of illite crystallinity, organic matter reflectance, and isotopic techniques to mineral exploration: A case study in southwestern Gaspé, Quebec. *Econ. Geol.* **1983**, *78*, 1350–1363.
62. Brauckmann, F.J. *Hochdiagenese im Muschelkalk der Massive von Bramsche und Vlotho*; Institut für Geologie, Ruhr-Universität Bochum: Bochum, Germany, 1984. (In German)
63. Bailey, S.W.; Brown, B.E. Chlorite polytypism: I. Regular and semi-random one layer structures. *Am. Mineral.* **1962**, *47*, 819–850.
64. Bailey, S.W. Classification and Structures of the Micas. In *Micas*; Bailey, S.W., Ed.; Mineralogical Society of America: Washington, DC, USA, 1984; pp. 1–12.
65. Hayes, J.B. Polytypism of chlorite in sedimentary rocks. *Clays Clay Miner.* **1970**, *18*, 285–306.